Role of Polymer Network and Gelation Kinetics on the Mechanical Properties and Adsorption Capacity of Chitosan Hydrogels for Dye Removal

Martina Salzano de Luna,[1,2] Rosaria Altobelli,[1] Lucia Gioiella,[1] Rachele Castaldo,[1,3] Giuseppe Scherillo,[1] Giovanni Filippone[1]

[1]Department of Chemical, Materials and Production Engineering (INSTM Consortium – UdR Naples), University of Naples Federico II, Piazzale Tecchio 80, 80125 Naples, Italy
[2]Institute for Polymers, Composites and Biomaterials, National Research Council of Italy, Piazzale E. Fermi 1, 80055, Portici (NA), Italy
[3]Institute for Polymers, Composites and Biomaterials, National Research Council of Italy, Via Campi Flegrei 34, 80078 Pozzuoli, Italy
Correspondence to: M. Salzano de Luna (E-mail: martina.salzanodeluna@unina.it) or G. Filippone (E-mail: gfilippo@unina.it)

ABSTRACT

Chitosan (CS) hydrogels are receiving growing attention as adsorbents for water purification purposes. The conditions of preparation of this class of materials play a crucial in the determination of their performances, however this aspect is often neglected in the literature. In this study we deal with this issue, focusing on the structure-property relationships of CS hydrogels obtained by phase inversion method. We show that the concentration of the starting solution determines the density and strength of intermolecular interactions, and that the gelation kinetics dictates the hydrogel structure at the microscale. Consequently, even subtle changes in the preparation protocol can cause significant differences in the performances of CS hydrogels in terms of mechanical properties and dye adsorption capacity. The observed trends are often neither trivial nor monotonic. Nonetheless, we demonstrate that they can be interpreted looking at the chitosan network structure, which can be inferred by rheological measurements.

KEYWORDS: hydrogels; structure-property relations; rheology; mechanical properties; dye adsorption

INTRODUCTION

Environmental pollution due to the disposal of large amounts of dye-bearing wastewater from tannery, textile, paper and pulp industries is a serious global issue. Nowadays, a great interest exists in identifying effective and low-cost adsorbents that do not represent an environmental problem by themselves.[1] Among the non-conventional materials which are being explored as potential eco-friendly solutions for water remediation, chitosan (CS)-based systems are receiving growing attention owing to their biocompatibility, biodegradability, relatively low cost, and high capacity and rate of adsorption of dyes and heavy metals.[2-4] A recent review by Liu and Bai deals with this subject, highlighting the areas in which further efforts are needed to ensure the effective applicability of CS-based materials in wastewater treatment.[5] In particular, the authors emphasize that a deeper understanding of the adsorption mechanisms is hoped for the optimization of the pollutant uptake capacity. Moreover, the possibility of reusing the adsorbent also appears to be a crucial aspect. In this regard, monolithic CS-based adsorbents are preferable compared to particulate systems, as they can be easily

separated from the liquid phase after the adsorption process, regenerated and eventually reused.[6-8] Among others, CS hydrogels, which in the last years have been mainly investigated for medical and pharmaceutical applications,[9-11] exhibit adequate mechanical properties and tunable adsorption capacity. Recent studies in this field mainly aimed at improving the adsorption performances via chemical modification of the CS chain and/or through the development of CS-based (nano)composites.[12-16] On the other hand, the conditions of preparation of CS hydrogels also affect the chain arrangement in the polymer network, thus playing a crucial role in determining the final properties of the adsorbent. Although widely recognized, the effect of the various processing parameters is seldom addressed. Among others, Mohamed et al.[17] and Cestari et al.[18] found that chemical cross-linking breaks intermolecular H-bonding between CS chains. As a result, increasing the amount of cross-linker brings about an increase of the accessible CS surface groups, thus determining a considerable improvement of its adsorption properties.[17] In contrast, Zhao et al. reported an inverse relationship between adsorbent capacity and concentration of the alkaline bath used to induce physical gelation in CS hydrogel beads.[19] It is evident the need for systematic studies aimed at shedding light on the complex relationships among chain arrangement in the polymer network at the molecular scale, hydrogel microstructure, and macroscopic

properties of CS hydrogels. Here, we address this issue by investigating in detail the effect of two relevant parameters, namely the CS concentration in solution and the gelation kinetics, on the mechanical properties and adsorption capacity of CS hydrogels towards anionic and cationic organic dyes. A thorough characterization of the samples was carried out from the sol- to the gel-state. We show that the mechanical and adsorption performances of CS hydrogels are strictly related to the structure of the CS network in the initial solution, which can be profitably monitored via rheological analysis. The obtained results demonstrate that the physico-chemical properties of CS hydrogels are highly sensitive to conditions of preparation, which thus need to be carefully controlled for a targeted design of this class of bio-sorbents.

EXPERIMENTAL

Materials

Medium molecular weight chitosan powder with deacetylation degree of 77±2% (Supporting Information, Section S1), Indigo Carmine (IC) and Rhodamine 6G (RH) dyes were purchased from Sigma Aldrich and used without further purification.

Hydrogel Preparation

The basic steps of the procedure for the preparation of the chitosan hydrogels are depicted in Figure 1.
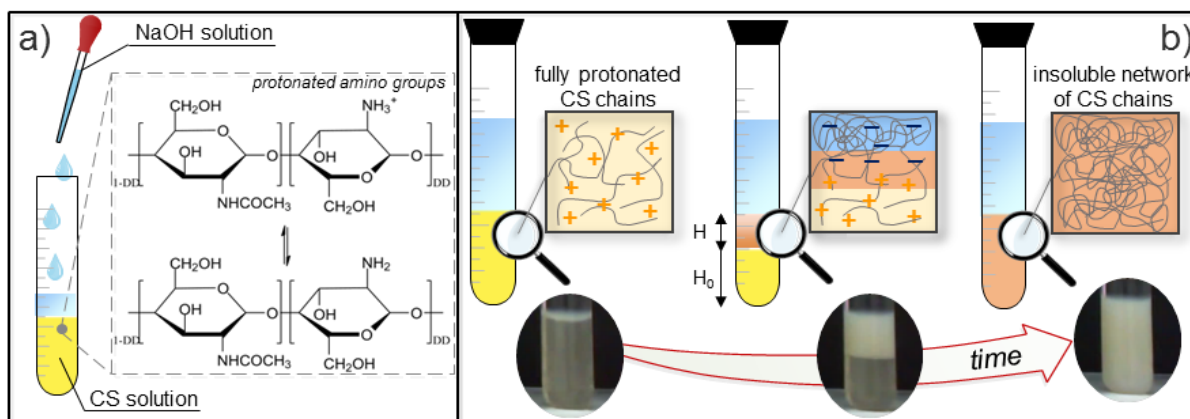
FIGURE 1 Preparation process of the chitosan hydrogels.

CS was dissolved in a 98/2 v/v% mixture of bi-distilled water and acetic acid via magnetic stirring at room temperature for 72 h. The hydrogels were obtained by the "phase inversion method", which consists in a direct but controlled exposure of the CS solution to an alkaline medium.[20,21] In this procedure, the hydrogel assembly is obtained by modifying the balance between hydrophilic and hydrophobic interactions in the CS solution.[22] Specifically, the local pH change in the CS solution during the diffusion of the alkaline species induces the formation of physical junctions due to hydrophobic interactions involving N-acetyl groups and hydrogen bonding among CS chains. In detail, 2 mL of CS solution were poured into glass test tubes, and an aqueous solution of sodium hydroxide (NaOH, 2 or 6 w/v%) was carefully poured on the top by using a needle so as not to disturb the liquid/liquid interface and to ensure a regular diffusion through it (Figure 1a). The volume ratio of CS:NaOH solutions was set to 1:1 for all the experiments. The formation of a physical network of CS chains proceeds over time from the liquid-liquid interface towards the bottom of the glass tube, following the diffusion of the alkaline species in the CS solution driven by the concentration gradient (Figure 1b). At the end of the process the CS hydrogels were collected, cut into cylindrical specimens (diameter 10 mm, thickness 4 mm), extensively rinsed with bi-distilled water until reaching neutral pH, and stored in water.

Hydrogel Characterization

The rheological properties of the CS solutions were measured by means of a stress-controlled rotational rheometer (ARG2, TA Instruments) in cone-plate geometry (diameter 40 mm, angle 2°) with a Peltier base for temperature control. The steady-shear viscosity, η, was measured at 25°C and three independent measurements were carried out for each sample. The CS gelation process was carried out in a climatic chamber that allows the accurate control of the temperature (set to 25°C). Since the gelled CS exhibits a brighter color compared to the not

gelled material, the gelation kinetics was easily monitored by referring to the progress of the relative position of the gelation front, λ, defined as $\lambda = H/H_0$ (see Figure 1b).[23] Thus, $\lambda = 1$ corresponds to the gelation of the whole CS solution contained into the glass test tube. Pictures were taken at regular time steps throughout the process. The images were analyzed using the open source image processing software ImageJ®. Five independent measurements were carried out for each sample. The morphology of the hydrogels was investigated by scanning electron microscopy (SEM) using a FEI Quanta 200 FEG SEM in high vacuum mode. Freeze-dried samples were cryo-fractured and sputter coated with a 15 nm thick Au–Pd layer. The observations were carried out at 10 kV acceleration voltage using a secondary electron detector. The mechanical behavior of the hydrogels in the swollen state was investigated by unconfined compression tests on cylindrical-shaped specimens (cross section A_0, height h_0) fully immersed in bi-distilled water. The samples were squeezed at a controlled speed of 5 μm s^{-1}, and the normal force, F_N, and the plate displacement, Δh, were recorded during time. The engineering stress, σ, and strain, ε, were calculated as $\sigma = F_N/A_0$ and $\varepsilon = \Delta h/h_0$.[24] The compressive modulus, E_c, was estimated in the linear region of the stress-strain curve. Ten independent measurements were carried out for each system. The statistical significance of the results was assessed by t-test. The swelling degree, SD, and porosity, P, of the neutralized hydrogels were calculated from the weight change before and after drying by using the following equations:[19]

$$SD = \frac{W_{wet} - W_{dry}}{W_{dry}} \cdot 100\% \tag{1}$$

$$P = \frac{W_{wet} - W_{dry} / \rho_{water}}{W_{dry} / \rho_{CS} + W_{wet} - W_{dry} / \rho_{water}} \% \tag{2}$$

where W_{wet} and W_{dry} represent the weight of the wet (chitosan hydrogels fully swollen in bi-distilled water) and dry samples, and ρ_{water} and ρ_{CS} are the density of water (1.0 g cm^{-3}) and CS (1.4 g cm^{-3}).[25] Five independent measurements

were carried out for each system. The adsorption behavior of the samples was investigated through batch adsorption tests from mono-component solutions of dye at different concentration (20-500 mg L^{-1}). Preliminary analyses with solutions at dye concentration of 100 mg L^{-1} were performed to estimate the time needed to reach equilibrium conditions (Supporting Information, Section S2). For each equilibrium adsorption experiment, a sample of 10 mg of hydrogel (dry basis with respect to chitosan) was added to a glass flask containing the dye solution (initial concentration, C_0). The flasks were stirred at 150 rpm and T = 25°C using a thermostated agitator (SKI 4, Argo Lab). The dye concentration in solution (equilibrium concentration, C_e) was measured with a spectrophotometer referring to the characteristic maximum absorbance wavelength of each dye (611 nm for IC and 527 nm for RH). All the experiments were carried out in replicate, and blanks were performed. The equilibrium adsorption capacity, q_e, was determined as:

$$q_e = \frac{C_0 - C_e}{m} \cdot V \qquad (3)$$

where m is the amount of dry CS hydrogel and V is the total volume of dye solution. The CS samples collected at the end of the adsorption tests were immersed in a fixed volume (50 mL)

of fresh bi-distilled water and kept in quiescent conditions at T = 25°C. The concentration of spontaneously released dye was measured every two days. The reported data refer to equilibrium conditions, which were considered attained when no differences among three consecutive measurements were found.

RESULTS AND DISCUSSION

Rheological properties of solutions and gelation kinetics

The steady-shear flow curves of a set of solutions at different CS concentration, C_{CS}, are shown in Figure 2a. The viscosity of the solutions increases with the CS content, and the shear-thinning feature becomes more accentuated. Fitting the Carreau-Yasuda model[26] to the experimental data allows the estimate of the zero-shear rate viscosity, η_0, which was used to compute the zero-shear rate specific viscosity, $\eta_{sp,0} = (\eta_0 - \eta_s)/\eta_s$, where η_s represents the solvent viscosity. The latter is reported in Figure 2b as a function of C_{CS}. Two distinct regimes can be identified, each characterized by a power-law dependence of $\eta_{sp,0}$ on C_{CS}. The rheological transition reflects entanglement effects and self-association of the CS chains occurring at sufficiently high polymer concentrations.[27,28]
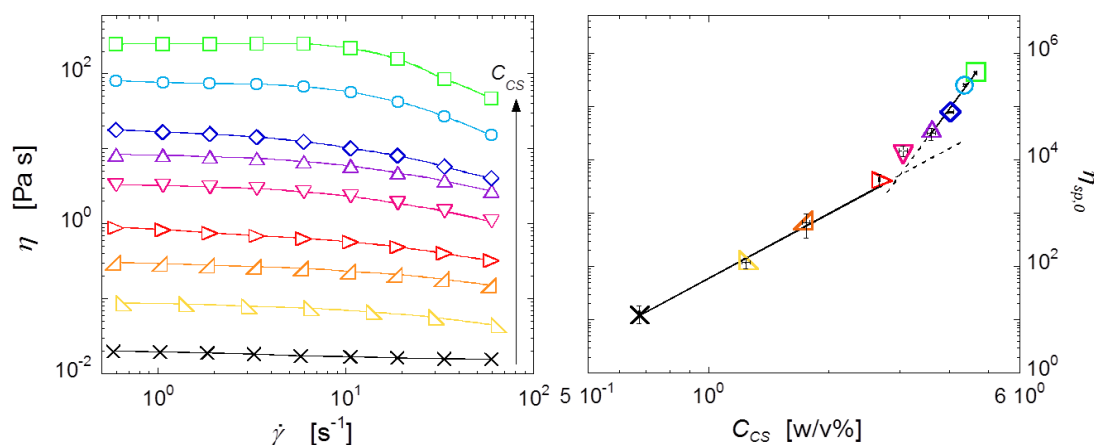

FIGURE 2 (a) Flow curves of solutions at different CS concentration (from bottom to top: C_{CS} = 0.67, 1.24, 1.75, 2.67, 3.06, 3.59, 4.03, 4.37, 4.64 w/v%). (b) Zero-shear specific viscosity as a function of CS concentration in solution.

The value of C_{CS} at which the system evolves from a solution of independently moving polymeric coils to an entangled chain network is generally referred as overlap concentration, C^*, and it can be determined by the intersection of the linear branches corresponding to the power-law correlations of $\eta_{sp,0}(C_{CS})$ in the two regimes.[29] In this way we have found $C^* \approx 3.2$ w/v%. The different intermolecular interactions which establish in CS solutions below and above C^* are expected to reflect in different structures of the resulting hydrogels. To study how this aspect affects the hydrogel performances, we prepared samples starting from solutions at C_{CS} = 3, 3.5 and 4 w/v%.

Another parameter that affects the hydrogel performances is the concentration of NaOH in the solution used to induce gelation, C_{NaOH}. The alkaline species diffuse in the CS solution due to the concentration gradient, causing the precipitation of an insoluble network of CS chains. The rate of such a process, which determines the structure of the CS network in the hydrogel, is a function of C_{NaOH}. This is shown in Figure 3a, where the time evolution of the relative position of the gelation front is reported for two samples at C_{CS} = 3 w/v% obtained using NaOH solutions at different concentration. For a fixed value of C_{CS}, the more concentrated the alkaline solution is, the faster is the advancement of the relative position of

the gelation front. A complex relationship exists between gelation kinetics and concentration of CS and NaOH. Three main phenomena occur during the gelation process: (1) mass transport of the alkaline species towards the surface of the CS solution; (2) diffusion of the alkaline species through the polymeric system (from the top to the bottom of the glass tubes shown in Figure 1b); (3) chemical reaction between the alkaline species and the amino groups on the CS chains, which are gradually deprotonated by the OH$^-$ from their initial protonated form in acidic environment.[23] The driving force of gelation is the molar ratio between the OH$^-$ ions in the NaOH solution and the $(-NH_3)^+$ groups in the CS one. The half-gelation time, $t_\lambda/2$, defined as the time needed to turn half of the initial solution depth into a gelled system, is reported as a function of the molar ratio between OH$^-$ ions and $(-NH_3)^+$ groups in Figure 3b (calculations are provided as Supporting Information, Section S3). Two clusters of data can be identified by referring to the value of C_{NaOH}. The latter parameter is much more relevant than C_{CS} in determining the kinetics of gelation, at least in the investigated range of CS concentration. Therefore, two solutions at C_{NaOH} =2 and 6 w/v% were selected to investigate the effect of a "slow" and "fast" gelation process on the performances of the CS hydrogels.
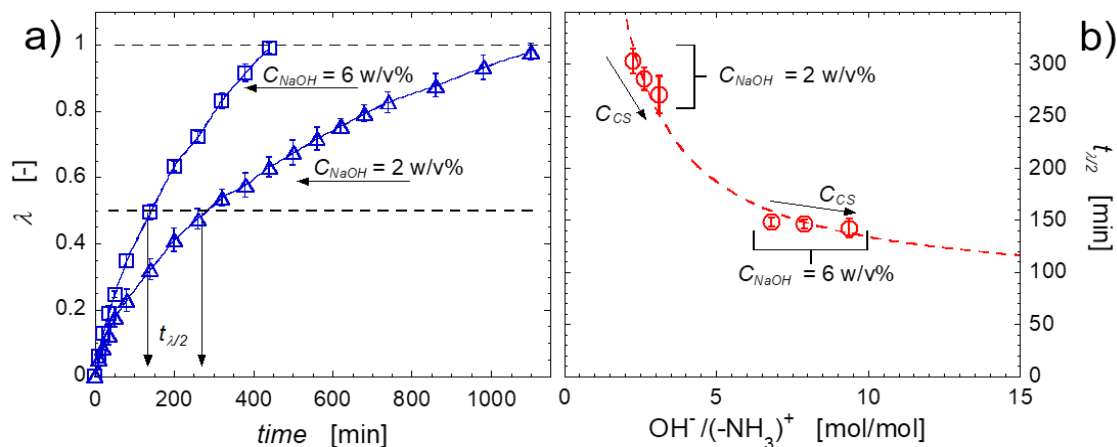

FIGURE 3 (a) Time evolution of the position of the gelation front for the solution at C_{CS} = 3 w/v%. (b) Half-gelation time as a function of the molar ratio between the alkaline species and the protonated amino groups of chitosan. Lines are guides for the eye.

Mechanical properties

CS hydrogels intended to be used as dye adsorbent materials should exhibit adequate mechanical resistance to allow for easy handling, recovery, and possible reuse of the samples.[2,30] Uniaxial unconfined compression tests were performed to compare the mechanical strength of the samples obtained in different conditions. Representative stress-strain curves are reported in Figure 4. All the samples share the same overall behavior under compression: the stress, initially low, exponentially grows with deformation. It is worth noting that no mechanical failure (i.e. hydrogel fracture) or cracking in the samples can be observed, even when they are compressed by 70%. The elastic compressive modulus was computed by neglecting the data at $\varepsilon < 0.05$, which are meaningless due to irregularities of the sample surface.[31] The inset of Figure 4 shows that E_c exhibits power-law dependence on C_{CS}. This reveals a direct relationship between the modulus and the density of "elastically active" CS chains in the hydrogel, which is in agreement with the theory of rubber elasticity.[32] The effect of C_{NaOH} is negligible, at least when hydrogels from CS solutions at $C_{CS} > C*$ are considered. Such a finding is in line with recent results by Takara et al. on the Young's modulus of CS films.[33] It can be argued that the network structure above the overlap concentration is stable enough not to be appreciably altered by the rate of pH-induced gelation. On the contrary, the value of C_{NaOH} determines a statistically significant difference in the E_c of the hydrogel prepared from the solution at $C_{CS} = 3$ w/v%. In this case the polymeric network is more loose, and carrying out a "slow" ($C_{NaOH} = 2$ w/v%) or "fast" ($C_{NaOH} = 6$ w/v%) gelation process affects the structure and, hence, the mechanical properties of the resulting hydrogel. In particular, E_c of the sample obtained using the solution at $C_{NaOH} = 6$ w/v% is ~40% higher than that of the sample prepared at $C_{NaOH} = 2$ w/v%. SEM analyses performed on the freeze-dried hydrogels shed light on this result (see Figure 5). The microstructure of the hydrogel obtained at $C_{NaOH} = 2$ w/v% consists of large (tens of microns) and irregularly-sized pores with continuous and homogeneous CS walls. In contrast, the sample obtained at $C_{NaOH} = 6$ w/v% appears more compact at the macro-scale (Figure 5c vs. 5a), but the image at higher magnification reveals that it is made of highly interconnected and small (few microns) pores (Figure 5d). It is thus not surprising that the thicker mesh of CS filaments obtained through the "fast" gelation process ($C_{NaOH} = 6$ w/v%) is more effective in bearing external stresses than the open and thin microstructure obtained via "slow" gelation ($C_{NaOH} = 2$ w/v%).
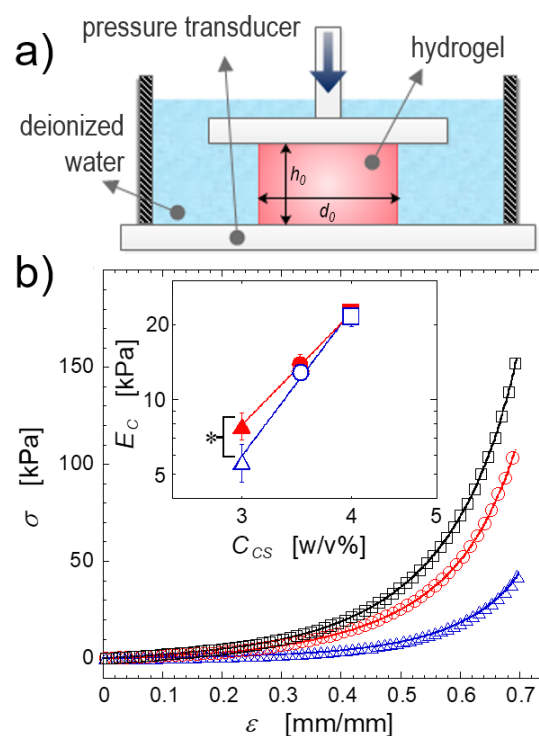

FIGURE 4 (a) Experimental setup. (b) Compressive stress-strain curves of the hydrogels at prepared from solutions at $C_{CS} = 3$ (triangles), 3.5 (circles) and 4 (squares) w/v% and $C_{NaOH} = 2$ w/v%. In the inset, the compressive modulus of hydrogels prepared at at $C_{NaOH} = 2$ (empty symbols) and 6 (full symbols) w/v% is shown as a function of C_{CS}. The asterisk indicates significant difference (p < 0.05) between the two series of data.
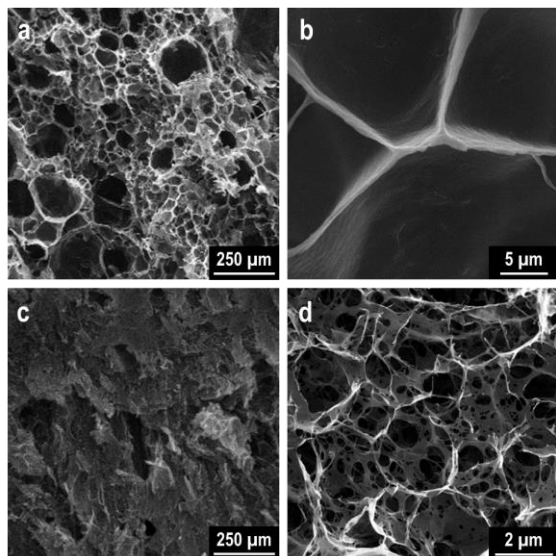
FIGURE 5 SEM micrographs of the freeze-dried hydrogels at C_{CS} = 3 w/v% and C_{NaOH} = (a ,b) 2 and (c, d) 6 w/v%.

Dye adsorption capacity

The equilibrium adsorption data of the CS hydrogels prepared in different conditions are shown in Figure 6. For all the systems, the Freundlich isotherm model[34] was found to well describe the dependence of the equilibrium adsorption capacity on the dye concentration (details are provided in the Supporting Information, see Section S4). The first general comment concerns the comparison between the two dyes. The uptake capacity of the CS hydrogels for IC is considerably higher than that for RH. This reflects the higher affinity of CS towards anionic species compared to cationic ones, at least when a fraction of the amino groups of the CS chain are in the protonated state.[35]
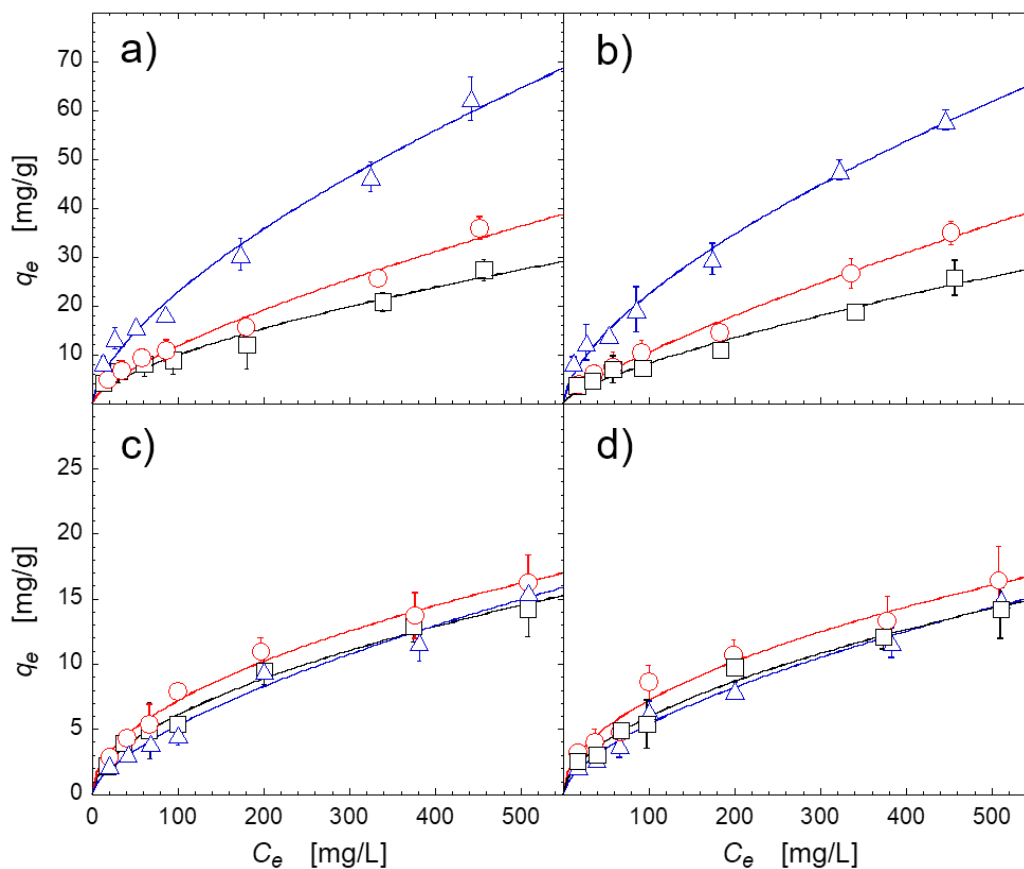
FIGURE 6 Adsorption equilibrium capacity respect to IC (a, b) and RH (c, d) for hydrogels at C_{CS}=3 (triangles), 3.5 (circles) and 4 (squares) w/v% and C_{NaOH}=2 (a, c) and 6 w/v% (b, d). Solid lines are the best fitting of the Freundlich isotherm model.

At neutral pH, ~50% of total chitosan amino groups are protonated.[2,30] As a consequence, the anionic IC molecules penetrate into the polymeric network of the hydrogel and adsorb on the CS chains thanks to electrostatic interactions occurring between the negatively charged sulfonate groups of the dye and the protonated amino groups of the polymer. In contrast, cation-cation repulsion limits the adsorption capacity of the hydrogels towards RH. The different CS-dye affinity was confirmed by release tests, which consisted in soaking the samples at the end of the adsorption tests in a known volume of fresh bi-distilled water and measuring the amount of dye spontaneously released in quiescent conditions. The results are shown in Figure 7 for a representative sample. Almost half of the adsorbed RH is released at equilibrium, while the amount of released IC is less than 10%. Dealing with dyes exhibiting different affinity allows us to examine in depth the effect of the preparation conditions on the adsorption behavior of the hydrogels.
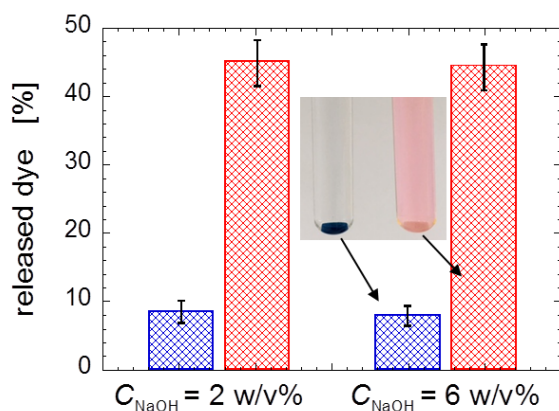
FIGURE 7 Percentage amount of spontaneously released IC (blue bars) and RH (red bars) dyes molecules by the CS hydrogels at C_{CS} = 3.5 w/v% soaked in a fixed volume of fresh water. Two representative samples are shown in the picture.

Figure 6 indicates that C_{NaOH} does not affect the adsorption capacity, and this holds true irrespective of the specific CS-dye affinity. This result is not trivial, as Figure 5 clearly shows that the concentration of the alkaline solution affects the hydrogel macro- and microstructure. Such a result suggests that the length scale more relevant in terms of adsorption capacity is the molecular scale. The latter is more strictly related to C_{CS}, which dictates the arrangement of the CS chains in the polymeric network. In fact, an increase in C_{CS} brings about a significant reduction of q_e for IC, i.e. the more affine dye. The decrease is particularly pronounced when passing from C_{CS} = 3 to 3.5 w/v%, while rising the CS concentration from 3.5 to 4 w/v% has a minor effect. This is in line with rheological analysis, which revealed a transition at $C_{CS} = C^*$ ≈ 3.2 w/v% due to the switch from diluted to concentrated regime (see Figure 2). Note that, as shown in Table 1, possible effects due to a different swelling degree or porosity of the samples can be excluded. This is not unexpected, as neither SD nor P easily correlate with the arrangement of the polymer chains in the network.

TABLE 1 Swelling degree and porosity of the hydrogels.

	C_{NaOH} = 2		C_{NaOH} = 6	
C_{CS}	SD [%]	P [%]	SD [%]	P [%]
3	2232±143	96.9±0.2	2255±60	97.1±0.1
3.5	2220±103	96.9±0.1	2189±83	96.8±0.1
4	2179±85	96.5±0.1	2114±78	96.4±0.1

To sum up, the results of Figure 6 indicate that the effectiveness of the functional groups of CS chains in trapping affine dye molecules can be fully exploited only at $C_{CS} < C^*$, i.e. when the polymer network is sufficiently loose at the molecular scale to favor solvent-dye exchange. Differently, the stronger intermolecular interactions that establish above C^* limit the adsorption ability of the CS chains (C_{CS} = 3.5 and 4 w/v%). Interestingly, Cestari *et al.* emphasized that dye and polymer have to lose part of their hydration shell so that dye adsorption can take place.[18] In line with this picture, the polymer network in the studied systems has to be loose

enough to allow for dye-solvent exchange. The importance of an appropriate choice of C_{CS} in the protocol for the preparation of CS hydrogels clearly emerges when comparing the IC adsorption capacity of our samples with literature data. Prado et al. found that the maximum quantity of IC absorbable by pristine CS powder is ~72 mg/g,[36] which is quite close to the value that we have found at C_{CS} = 3 w/v%. Hence, it is worth noting that a non-optimized choice of C_{CS} can have a strongly negative impact on the adsorption capacity, which almost halves when C_{CS} is increased from 3 to 3.5 w/v%. On the other hand, the preparation conditions play a minor role in terms of adsorption capacity when a non-affine dye such as RH is considered. In this case the adsorption capacity is low irrespective of density and strength of intermolecular interactions (C_{CS}) and rate at which gelation is induced (C_{NaOH}).

CONCLUSIONS

Chitosan hydrogels were obtained by a controlled exposure of a CS solution to an alkaline (NaOH) medium (phase inversion method). The role of the preparation conditions on the macroscopic performances of the hydrogels was studied. The CS concentration in the starting solution and the gelation kinetics were found to significantly influence the chain arrangement in the polymer network at the molecular scale, as well as the hydrogel micro- and macro-structure. As a result, even subtle changes in the preparation protocol can cause significant differences in the properties of the CS hydrogels. The observed trends resulted neither trivial nor monotonic, and they were related to the structure of the CS network in the hydrogels. Rheological characterization of the starting CS solutions provided valuable information about the chain arrangement in the resulting hydrogel, revealing to be a useful complementary tool for the study of this class of materials. The overlap concentration of CS in solution (i.e. the boundary concentration between dilute and concentrated regime) was found to play a crucial role in determining the

mechanical properties and adsorption ability of the hydrogels. In particular, the samples prepared from solutions at C_{CS} below C^* exhibited high adsorption capacity towards chemically affine dyes and a compressive modulus dependent on the gelation kinetics. A low sensitivity of the hydrogel performances to the conditions of preparation was instead noticed for the hydrogel obtained from more concentrated CS solutions. The results were interpreted in the framework of the literature addressing the role of solute-solute and solute-solvent interactions. Overall, our study highlight the relevance of a fine tuning of the conditions of preparation of CS hydrogels intended for dye removal applications.

REFERENCES

1. G. Crini, *Bioresource Technol.* **2006**, *97*, 1061-1085.
2. G. Crini, P. M. Badot, *Prog. Polym. Sci*. **2008**, *33*, 399-447.
3. M. Vakili, M. Rafatullah, B. Salamatinia, A. Z. Abdullah, M. H. Ibrahim, K. B. Tan, Z. Gholami, P. Amouzgar, *Carbohyd. Polym.* **2014**, *113*, 115-130.
4. S. Olivera, H. B. Muralidhara, K. Venkatesh, V. K. Guna, K. Gopalakrishna, Y. Kumar, *Carbohyd. Polym.* **2016**, *153*, 600-618.
5. C. Liu, R. Bai, *Curr. Opin. Chem. Eng.* **2014**, *4*, 62-70.
6. V. M.Esquerdo, T. R. S. Cadaval, G. L. Dotto, L. A. A. Pinto, *J. Colloid Interf. Sci.* **2014**, *424*, 7-15.
7. T. V. Rêgo, T. R. S. Cadaval, G. L. Dotto, L. A. A. Pinto, *J. Colloid Interf. Sci.* **2013**, *411*, 27-33.
8. G. L. Dotto, J. M. D. Moura, T. R. S. Cadaval, L. A. A. Pinto, *Chem. Eng. J.* **2013**, *214*, 8-16.
9. B. Hexig, H. Alata, Y. Inoue, *J. Polym. Sci., Part B: Polym. Phys.* **2005**, *43*, 3069-3076.
10. N. Bhattarai, J. Gunn, M. Zhang, *Adv. Drug Deliv. Rev.* **2010**, *62*, 83-99.

11. D. J. Overstreet, D. Dutta, S. E. Stabenfeldt, B. L. Vernon, *J. Polym. Sci., Part B: Polym. Phys.* **2012**, *50*, 881-903.

12. J. O. Gonçalves, J. P. Santos, E. C. Rios, M. M. Crispim, G. L. Dotto, L. A. A Pinto, *J. Molec. Liq.* **2017**, *225*, 265-270.

13. X. Wang, Y. Zheng, A. Wang, *J. Hazard. Mater.* **2009**, *168*, 970-977.

14. Y. Haldorai, J. J. Shim, *Appl. Surf. Sci.* **2014**, *292*, 447-453.

15. A. Vanamudan, K. Bandwala, P. Pamidimukkala, *Int. J. Biol. Macromol.* **2014**, *69*, 506-513.

16. G. J. Copello, A. M. Mebert, M. Raineri, M. P. Pesenti, L. E. Diaz, *J. Hazard. Mater.* **2011**, *186*, 932-939.

17. M. H. Mohamed, I. A. Udoetok, L. D. Wilson, J. V. Headley, *RSC Adv.* **2015**, *5*, 82065-82077.

18. A. R. Cestari, E. F. Vieira, A. M. Tavares, R. E. Bruns, *J. Hazard. Mater.* **2008**, *153*, 566-574.

19. F. Zhao, B. Yu, Z. Yue, T. Wang, X. Wen, Z. Liu, C. Zhao, *J. Hazard. Mater.* **2007**, *147*, 67-73.

20. K. Yao, J. Li, F. Yao, Y. Yin, Chitosan-based hydrogels: functions and applications, CRC Press, **2011**.

21. S. Ladet, L. David, A. Domard, *Nature* **2008**, *452*, 76.

22. A. Montembault, C. Viton, A. Domard, *Biomaterials* **2005**, *26*, 933-943.

23. A. Venault, D. Bouyer, C. Pochat-Bohatier, L. Vachoud, C. Faur, *AIChE J.* **2012**, *58*, 2226-2240.

24. J. Tang, M. A. Tung, Y. Zeng, *Carbohyd. Polym.* **1996**, *29*, 11-16.

25. T. Uragami, T. Matsuda, H. Okuno, T. Miyata, *J. Membr. Sci.* **1994**, *88*, 243-251.

26. P. J. Carreau, *Trans. Soc. Rheol.* **1972**, *16*, 99-127.

27. J. Desbrieres, *Biomacromolecules* **2002**, *3*, 342-349.

28. M. M. Amiji, *Carbohyd. Polym.* **1999**, *26*, 211-213.

29. R. Lapasin, S. Pricl, Rheology of industrial polysaccharides: Theory and applications, Springer, US, **1995**.

30. G. L. Dotto, J. M. D. Moura, T. R. S. Cadaval, L. A. A. Pinto, *Chem. Eng. J.* **2013**, *214*, 8-16.

31. E. C. Muniz, G. Geuskens, *Macromolecules* **2001**, *34*, 4480-4484.

32. K. S. Anseth, C. N. Bowman, L. Brannon-Peppas, *Biomaterials* **1996**, *17*, 1647-1657.

33. E. A. Takara, J. Marchese, N. A. Ochoa, *Carbohyd. Polym.* **2015**, *132*, 25-30.

34. H. M. F. Freundlich, *J. Phys. Chem.* **1906**, *57*, 1100.

35. G. Z. Kyzas, N. K. Lazaridis, *J. Colloid Interf. Sci.* **2009**, *331*, 32-39.

36. A. G. Prado, J. D. Torres, E. A. Faria, S. C. Dias, *J. Colloid Interf. Sci.* **2004**, *277*, 43-47.